Feedback Network Controls Photoreceptor Output at the Layer of First Visual Synapses in *Drosophila*

Lei Zheng,[1] Gonzalo G. de Polavieja,[2,3] Verena Wolfram,[1] Musa H. Asyali,[4] Roger C. Hardie,[5] and Mikko Juusola[1]

[1]Department of Biomedical Science, University of Sheffield, Sheffield S10 2TN, UK
[2]Department of Theoretical Physics, Universidad Autónoma de Madrid, 28049 Spain
[3]Instituto Nicolás Cabrera de Física de Materiales, Universidad Autónoma de Madrid, 28049 Spain
[4]Faculty of Engineering and Architecture, Yasar University, Izmir, Turkey
[5]Department of Anatomy, University of Cambridge, Cambridge CB2 3DY, UK

At the layer of first visual synapses, information from photoreceptors is processed and transmitted towards the brain. In fly compound eye, output from photoreceptors (R1–R6) that share the same visual field is pooled and transmitted via histaminergic synapses to two classes of interneuron, large monopolar cells (LMCs) and amacrine cells (ACs). The interneurons also feed back to photoreceptor terminals via numerous ligand-gated synapses, yet the significance of these connections has remained a mystery. We investigated the role of feedback synapses by comparing intracellular responses of photoreceptors and LMCs in wild-type *Drosophila* and in synaptic mutants, to light and current pulses and to naturalistic light stimuli. The recordings were further subjected to rigorous statistical and information-theoretical analysis. We show that the feedback synapses form a negative feedback loop that controls the speed and amplitude of photoreceptor responses and hence the quality of the transmitted signals. These results highlight the benefits of feedback synapses for neural information processing, and suggest that similar coding strategies could be used in other nervous systems.

The Journal of General Physiology

INTRODUCTION

Both in invertebrate compound eyes and in vertebrate retina, visual information is processed by interconnecting neurons that communicate with graded signals (Kaneko, 1979; Sterling, 1983; Meinertzhagen, 1993; Juusola et al., 1996; Wässle, 2004). Ultrastructural studies and neurochemistry have shown a complex arrangement of feedforward and feedback synapses that use a diverse array of excitatory and inhibitory transmitters. However, the understanding of this sophistication has been limited at best, in part because monitoring activity in vivo and asserting functions for individual parts of the network is very difficult.

To further our understanding of feedback synapses in visual processing, we have turned to a *Drosophila* preparation, whose genetics and modular eye morphology (Meinertzhagen and Sorra, 2001) offer clear advantages (Fig. 1 A). The ultrastructure of the first visual synaptic layer in *Drosophila* (Fig. 1 B) has been fully described from electron-micrograph sections (Meinertzhagen and O'Neil, 1991). The first optic neuropile, the lamina, is an assembly of stereotyped cartridges, neuro-ommatidia, where axon terminals of photoreceptors (R1–R6, one from each of six neighboring ommatidia) each make ~50 output synapses known as tetrad synapses (Meinertzhagen and O'Neil, 1991), a total of 283 in one complete reconstruction (Meinertzhagen and Sorra, 2001). Each of these contacts (Fig. 1 B, a) releases histamine (Hardie, 1989a; Gengs et al., 2002) onto two large monopolar cells (LMCs) and onto a fingerlike process of an amacrine cell, AC, that runs between two photoreceptor axons (Fig. 1 B). AC processes are linked together and to adjacent cartridges with thin extending fibers (Campos-Ortega and Strausfeld, 1973; Fischbach and Dittrich, 1989), suggesting that each process could be a locally interacting element, which may see only limited activity from other such segments in the same or neighboring cartridges (Shaw, 1984). In return, photoreceptor axons receive feedback from the primary visual interneurons (Meinertzhagen and Sorra, 2001): a total of 48 synapses from the ACs (Fig. 1 B, b) and 25 from LMCs (Fig. 1 B, c) (Meinertzhagen and Sorra, 2001). Although these are the only direct feedback connections to photoreceptor terminals, photoreceptor output may also be influenced indirectly via LMCs that receive lateral (L4) and centrifugal feedback from other cartridges (Fig. 1 B, D) and from higher processing centers (Fig. 1 B, e), respectively.

We have developed a new *Drosophila* preparation that allows long-lasting intracellular recordings from

Correspondence to Mikko Juusola: m.juusola@sheffield.ac.uk

The online version of this article contains supplemental material.

Abbreviations used in this paper: AC, amacrine cell; ERG, electroretinogram; LMC, large monopolar cell; NS, naturalistic stimulation; SNR, signal-to-noise ratio; WT, wild-type.

photoreceptors and LMCs in vivo. Using this preparation, we investigate the role of feedback circuitry in neural information processing by comparing voltage responses of photoreceptors and LMCs in wild-type (WT) flies and in synaptic mutants.

We use three specific mutants to work out the feedback dynamics: ort^{P306}, *ebony*, and temperature-sensitive $shibire^{TS1}$. According to in vitro experiments, LMCs of ort^{P306} have reduced sensitivity for histamine (Gengs et al., 2002), whereas *ebony* has impaired histamine recycling that reduces the available transmitter pool in photoreceptor axon terminals (Borycz et al., 2002). Both of these mutants should therefore reduce the probability for successful synaptic transmission from photoreceptors to the primary visual interneurons in vivo. Nonetheless, surprisingly our in vivo recordings show that voltage responses of ort^{P306} and *ebony* photoreceptors to light stimuli are larger and faster than those of WT flies, and that the rate of information transfer in ort^{P306} LMCs can reach that of WT LMCs at bright illumination. Hence the data from the synaptic mutants suggest that by boosting presynaptic responses visual signals can be made to cross the malfunctioning synapses. We then look for evidence for the mechanisms involved. In vitro patch-clamp data from dissociated photoreceptors, which lack axon terminals and thus any synaptic feedback, show that the response properties of ort^{P306} photoreceptors are identical to those of WT photoreceptors. Therefore, the differences in voltage responses of photoreceptors in vivo cannot be attributed to homeostatic mechanisms in the phototransduction or in the photoreceptor membrane properties. To resolve this matter we record in vivo from photoreceptors and LMCs of temperature-sensitive $shibire^{TS1}$ mutants. We show that warming $shibire^{TS1}$ above 28°C silences all vesicle-driven synaptic transmission between their photoreceptors and primary visual interneurons, and that the voltage responses of WT photoreceptors are being boosted continuously by excitatory feedback from the interneurons. When the signal transfer from photoreceptors to LMCs is low, as is the case in dim conditions, or compromised, as in mutants like ort^{P306} and *ebony*, the synaptic feedback gets stronger to boost photoreceptor output, increasing the probability for successful synaptic transmission to the primary visual interneurons.

We present our findings in two parts. First, recordings from ort^{P306}, *ebony*, and temperature-sensitive $shibire^{TS1}$ mutants provide strong evidence that synaptic feedback to photoreceptor terminals modulates the photoreceptor output. Second, using statistical methods, we provide evidence indicating that this modulation is predominantly from direct synaptic feedback and that it improves the signaling quality during naturalistic stimulation (NS). Based on the most dominant anatomical connections, we deduce the simplest negative feedback model that is sufficient to explain these findings. In this model, photoreceptor output to the interneurons is first sign-inverted and then fed back to photoreceptor terminals via excitatory synaptic conductances.

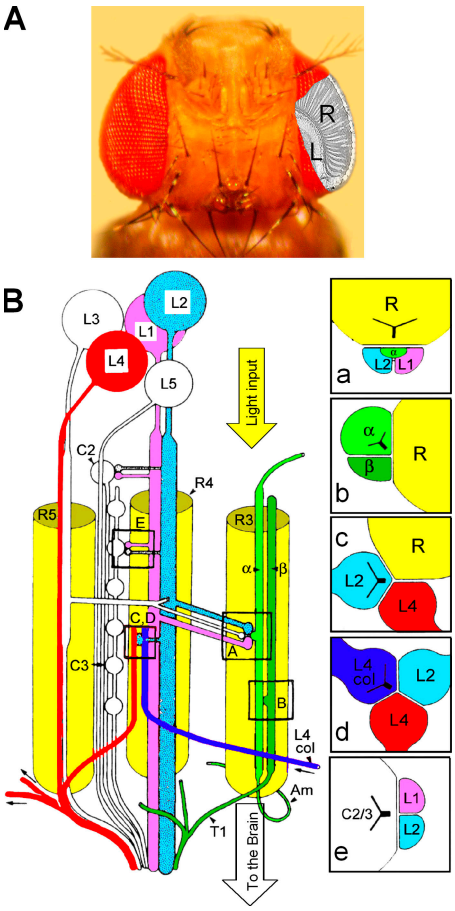

Figure 1. Location of the first visual synaptic layer and feedforward and feedback connections within a neuro-ommatidium. (A) Photo of *Drosophila* head with schematic cutaway view of retina, R, and lamina, L. (B) A greatly simplified view of neuro-ommatidial wiring (adapted from Meinertzhagen and O'Neil, 1991). Photoreceptor axon terminals, R1–R6 (three shown) form output synapses with five large monopolar cells (LMCs), L1–5, and an amacrine cell (AC), α. Inset a, tetrad synapse, a photoreceptor terminal connects to two LMCs and an AC. Insets b and c, feedback synapses from AC and L2 cell to a photoreceptor, respectively. Insets d and e, collaterals from other neuro-ommatidia.

MATERIALS AND METHODS

Flies

Wild type red-eyed Oregon (WT) flies, red-eyed ort^{P306} and $shibire^{TS1}$ mutants (Poodry et al., 1973; van der Bliek and Meyerowitz, 1991; Kawasaki et al., 2000; Kitamoto, 2001; Gengs et al., 2002), and *ebony* (*Drosophila melanogaster*) were raised on standard medium at 19°C in 12:12 light:dark cycle (Wolfram and Juusola, 2004). The flies were taken for in vivo experiments within 1–12 d and for in vitro patch-clamping a few hours after eclosion. We confirmed by sequencing that our ort^{P306} strain shared the same mutated base pairs as reported previously (Gengs et al., 2002).

In Vitro Electrophysiology

Whole-cell voltage-clamp recordings were made from WT and ort^{P306} photoreceptor somata to compare the phototransduction machinery and membrane properties of these cells. These recordings were used to test whether homeostatic mechanisms could enhance photoreceptor output when signal transmission to primary visual interneurons was compromised by faulty histamine (*ort*) receptors on post-synaptic LMCs. Dissociated ommatidia of recently eclosed flies were prepared and transferred to a recording chamber on an inverted Nikon Diaphot microscope (Hardie, 1991a). Experiments were performed within 2 h of eclosion, since photoreceptors do not readily dissociate at later times (Hardie, 1991b). The bath was composed of (in mM) 120 NaCl, 5 KCl, 10 TES, 4 $MgCl_2$, 1.5 $CaCl_2$, 25 proline, and 5 alanine. Recordings were done using Axopatch 1-D (Axon Instruments, Inc.) and electrodes of resistance ~10–15 MΩ; series resistance <25 MΩ and compensated to 80%. Light stimulation via a green LED was set to a maximum effective intensity of $\sim 2 \times 10^5$ photons/s per photoreceptor. Relative intensities were calibrated using a photomultiplier and converted to absolute intensities in terms of effectively absorbed photons by counting quantum bumps at low intensities (Hardie, 1991a).

In Vivo Experiments

We recorded voltage responses of photoreceptors and LMCs to identical light stimuli separately as the small cells make simultaneous recordings impractical. Intracellular recordings were made using sharp quartz microelectrodes (Juusola and Hardie, 2001a) (Sutter Instrument Co.) of resistance 120–200 MΩ at 25.0 ± 0.5°C. The intraelectrode solution was 3 M KCl for photoreceptor experiments; but 3 M potassium acetate with 0.5 mM KCl for LMCs to prevent rundown of the chloride battery (Hardie, 1989a). Responses were amplified by SEC-10L (NPI Electronic) in current-clamp mode using switching frequencies of ~15 kHz and low-pass filtered with light stimuli at 1.5 kHz (Kemo VBF8).

Similar to electrophysiological experiments in blowfly (*Calliphora vicina*) (Juusola et al., 1995), light responses from the cells of retina and lamina and their respective extracellular spaces show location-dependent, easily identifiable characteristics as the microelectrode advances in the tissue. The microelectrodes were guided through the small corneal openings with different entrance angles for photoreceptors and LMCs to facilitate the penetrations of the targeted cells (see Fig. 2).

When traveling in retina, microelectrodes penetrated alternatingly photoreceptors, glia, and intercellular space (Juusola et al., 1994; Juusola and Hardie, 2001a). Typically, the resting potentials of photoreceptors varied from −60 to −77 mV, while the intercellular space remained at zero, and glia potentials were below −85 mV. Bright light pulses evoked different responses from each of these cellular structures. Photoreceptors produced fast depolarizations of >40 mV, intercellular space showed slow hyperpolarizing field potentials to −8 mV, and maximum glia potentials were slow depolarizations <5 mV. All intracellular responses of photoreceptors of this study, apart from the photoreceptor axons shown in Fig. 9, were recorded in retina.

In the lamina, microelectrodes impaled photoreceptor axons, glia, intercellular space, and LMCs (and possibly ACs). The resting potential of photoreceptor axons varied from −65 to −80 mV, glia potentials were <−90 mV, laminal intercellular space was from −20 to −40 mV and LMCs were from −40 to −70 mV. All these values are given in respect to the intercellular space of retina (0 mV). Bright light pulses evoked different responses from laminal structures. Similar to data from *Calliphora* (Weckström et al., 1993; Juusola et al., 1995), voltage responses of photoreceptor axons showed a rapid prespike (Juusola and Hardie, 2001a) or an enhanced rise (Fig. 9) followed by 10–40 mV depolarization. As these responses deteriorated easily and were difficult to maintain for longer periods, their response statistics were not analyzed further. Glia cells produced very slow hyperpolarizations of few mV, whereas slow depolarizing field potentials could reach 15 mV. LMCs responded to light pulses with transient hyperpolarizations that could reach values of 45 mV. The large size, polarity, and rapid time course of these voltage responses closely resembled those of *Calliphora* LMCs, identified in previous electrophysiological and labeling studies (Juusola et al., 1995; Uusitalo et al., 1995). We made no attempt to characterize voltage responses of LMCs into subtypes.

Photoreceptors included in this study had resting potentials in darkness <−60 mV and maximum responses >40 mV (WT, ort^{P306}, and *ebony*) or >30 mV ($shibire^{TS1}$). WT, ort^{P306}, and $shibire^{TS1}$ LMCs had resting potentials <−40 mV and maximum responses >40 mV (WT), >15 mV (ort^{P306}), and >20 mV ($shibire^{TS1}$). The quality of recordings was high in these conditions.

Light Stimulation and Data Collection

Cells were stimulated at the center of their receptive fields by light from a high-intensity green LED (Marl Optosource, with peak emission at 525 nm) mounted on a cardan arm. The LED constituted a small field stimulus subtending 5° as seen by the fly. Such stimulus should be smaller than a typical receptive field of a *Drosophila* photoreceptor, whose half-width is estimated to be between 5° and 6° (Götz, 1964; Heisenberg and Buchner, 1977; Stavenga, 2003). The responsiveness of photoreceptors remained unchanged when stimulated with a small field light source that extended only 1°, as seen by the fly, indicating that during stimulation, lateral interactions were minimal (see Fig. S1 A, available at http://www.jgp.org/cgi/content/full/jgp.200509470/DC1). The LED output was taken as the light stimulus. It was measured by photodiodes both during 10-ms light pulses and during repetitions of a 1-s-long naturalistic light pattern (van Hateren, 1997; Juusola and de Polavieja, 2003). The naturalistic light pattern selected from the van Hateren natural stimulus collection, http://hlab.phys.rug.nl/archive.html (van Hateren, 1997), used fully the response ranges of the cells (30–60 mV, 2–200 Hz). The studied intensity range covered 4 log units (Juusola and Hardie, 2001a) from ~600 photons/s to $\sim 6 \times 10^6$ photons/s (I_0). Figures show results for dim (1,850 photons/s), medium (60,000 photons/s), and bright light (1.85×10^6 photons/s). Typically, cells were first studied at dim intensities before systematically proceeding to brighter stimulation. The stimulus and response were sampled at 10 kHz. Stimulus generation, data acquisition, and analysis were performed by Matlab interface BIOSYST (Juusola and Hardie, 2001a; Juusola and de Polavieja, 2003) with acquisition control via MATDAQ C-commands (H.P.C. Robinson, Cambridge Conductance).

Temperature Experiments

For temperature sensitivity tests, the voltage responses of 5–15-min dark-adapted photoreceptors to light pulses were first recorded at 18–20°C before warming up the flies (28–32°C) using a feedback-controlled Peltier-element embedded in the setup (Juusola and Hardie, 2001b). Additionally, the head temperature of the flies was measured with a separate thermocouple and the recordings were calibrated using these values (Juusola and Hardie, 2001b). The warming caused muscle activity that made intracellular recordings very challenging. However, occasionally (in four $shibire^{TS1}$ and five WT) we managed to record from the same photoreceptors without losing the penetration at different temperatures for several minutes (such as those shown in Fig. 6, C and D, and in Fig. S5, A and B). Other recordings, although requiring slight positional adjustments in the microelectrode to keep it intracellular, showed neither obvious differences in the findings nor in the quality of the data (Fig. S5, C and D). Furthermore, we frequently recorded electroretinograms (ERGs) of $shibire^{TS1}$ mutants to a saturating light pulse at 20°C and at 30°C in order to

confirm that warming removed the on- and off-transients, associated with synaptic transmission from photoreceptors to LMCs (Gengs et al., 2002) (Fig. S4).

Signal-to-Noise Ratio (SNR) Analysis

We analyzed the signaling performance of photoreceptor and LMC output by estimating their signal and noise components, and signal-to-noise ratios both in the time and frequency domain. The voltage responses were prepared for the analysis by removing the first 5–20 traces of response series to a repeated naturalistic stimulation to eliminate adaptational trends. The signal, $s(t)$, was then the average of the remaining voltage responses (typically >50 traces), whereas the noise traces, $n(t)_i$, were the difference between individual traces and the signal (Juusola et al., 1995).

Noise traces, $n(t)_i$, of photoreceptors were analyzed further to see whether they were purely random or whether they contained time-dependent features. The noise variance of photoreceptors (Juusola and de Polavieja, 2003) as shown in Fig. 7 E was taken at each time (or sampling) point across all the noise traces (0.1 ms resolution).

$SNR(t)$ in the time domain (Fig. 7 F) was calculated as the ratio between signal variance and noise variance, using 1-ms resolution. Fourier spectra of $s(t)$ and $n(t)$, i.e., $S(f)$ and $N(f)$, respectively, were calculated using 1 kHz sampling. Dividing $S(f)$ by the corresponding $N(f)$ gave the signal-to-noise ratio in the frequency domain (Shannon, 1948; Juusola and de Polavieja, 2003), $SNR(f)$. In general, the SNR analysis gives an approximation of the signaling performance of the neurons, as their signal and noise are not purely additive, nor is their dynamics Gaussian (Shannon, 1948; Juusola and de Polavieja, 2003).

Calculating the Rate of Information Transfer

We used the triple extrapolation method (Juusola and de Polavieja, 2003) to calculate the rate of information transfer for photoreceptor and LMC voltage responses. The triple extrapolation method, unlike SNR analysis, requires no assumptions about the signal and noise distributions or their additivity (Juusola and de Polavieja, 2003). Some practical considerations for the analysis are as follows. Only cells that allowed stable recordings at eight or nine light intensity levels were selected for analysis. For both WT and ort^{P306} photoreceptors, we had seven complete recording series. For WT LMCs we used two complete series and one for an ort^{P306} LMC. Numerous recordings from WT and ort^{P306} photoreceptors and LMCs obtained at particular light levels behaved similarly to the corresponding ones in the complete series. After removing the first 5–20 trials that showed a strong adaptational trend, we typically used the next 50 traces. The voltage response was resampled from 10 kHz to 1 kHz to remove high frequency noise, and a response matrix of 1,000 points × 50 trials was obtained for the analysis. The order of the trials was also shuffled to minimize the effect of any remaining adaptational trends (Juusola and de Polavieja, 2003). The total entropy and noise entropy were then obtained from the response matrices using the extrapolation parameters given in Table S2.

Online Supplemental Material

Supplemental material for this paper consists of five figures and two tables (available at http://www.jgp.org/cgi/content/full/jgp.200509470/DC1). Fig. S1 shows that neither lateral synaptic connections in lamina nor ERG are the cause for the peak in noise variance of photoreceptors. Fig. S2 shows the phototactic behavior of ort^{P306} and WT flies. Fig. S3 shows mean membrane potential of LMCs during long experiments in vivo. Fig. S4 shows typical ERG responses of WT flies and $shibire^{TS1}$ mutants. Fig. S5 shows voltage responses of $shibire^{TS1}$ and WT flies and their statistics. Table S1 gives light current statistics of WT flies and ort^{P306} mutants. Table S2 gives extrapolation parameters used for calculating the rate of information transfer.

RESULTS

To investigate the role of the feedback upon signal transfer across the first visual synapses we recorded intracellularly from photoreceptors and LMCs of wild-type (WT) and ort^{P306} mutant flies (Fig. 2 A). ort^{P306} is a hypomorph that expresses defective histamine receptors (ort^{P306} receptors) in LMCs and probably in ACs (Fig. 1 B, a), thus reducing the sensitivity of LMCs to histamine by at least 10-fold (Gengs et al., 2002). Therefore, if the presumed feedback originates from the interneurons whose responses are altered by this mutation, ort^{P306} photoreceptors should receive very different feedback from them. To observe this difference in feedback activity without exciting neighboring neuro-ommatidia, the light stimulus was delivered within the receptive field of a single photoreceptor (Fig. 1 B, d and e; Fig. S1 A). Since it is possible that the reduced sensitivity of histamine receptors could render the ort^{P306} mutant blind (Gengs et al., 2002), this experiment (Fig. 2 A) should also reveal whether its LMCs, in fact, can convey any visual signals toward the brain.

ort^{P306} Photoreceptors Show Enhanced Responsiveness

The lower half of Fig. 2 shows the recording settings (Fig. 2, B and C) as well as typical pre (R1–R6; Fig. 2, D and F) and postsynaptic (LMC; Fig. 2, E and G) voltage responses of WT and ort^{P306} mutant flies to a dim, medium, and bright intensity pulse. As in larger flies (Järvilehto and Zettler, 1971; Srinivasan et al., 1982; Laughlin et al., 1987; Srinivasan et al., 1990; van Hateren, 1992; Juusola et al., 1995; de Ruyter van Steveninck and Laughlin, 1996; van Hateren, 1997; van Hateren and Snippe, 2001), LMCs of WT *Drosophila* responded to photoreceptor depolarizations with a graded and phasic hyperpolarization (Fig. 2 E), mostly owing to histamine-gated chloride channels (Hardie, 1989a; Juusola et al., 1996; Gengs et al., 2002). As the speed and amplitude of presynaptic responses increased with the brightening stimulus (Fig. 2 D), the LMC output became increasingly transient, peaking before photoreceptor voltages (Fig. 2 H). In contrast, the responses of ort^{P306} photoreceptors and LMCs were different (Fig. 2, F and G). ort^{P306} photoreceptors generated faster (Fig. 2 H; red squares) and larger responses (Fig. 2 I) than WT photoreceptors (black squares) at all tested luminances apart from the brightest stimulation where the maximum amplitude of the responses saturated. While the responses of ort^{P306} and WT LMCs (Fig. 2 I, red circles) both increased with brighter stimulation, ort^{P306} responses remained smaller than the relatively constant-size WT responses (Fig. 2 I, black circles). Nevertheless, our data establishes that ort^{P306} LMCs generate a significant throughput for visual signals, responding better than might have been expected from their in vitro histamine sensitivity (Gengs et al., 2002), especially at bright luminances.

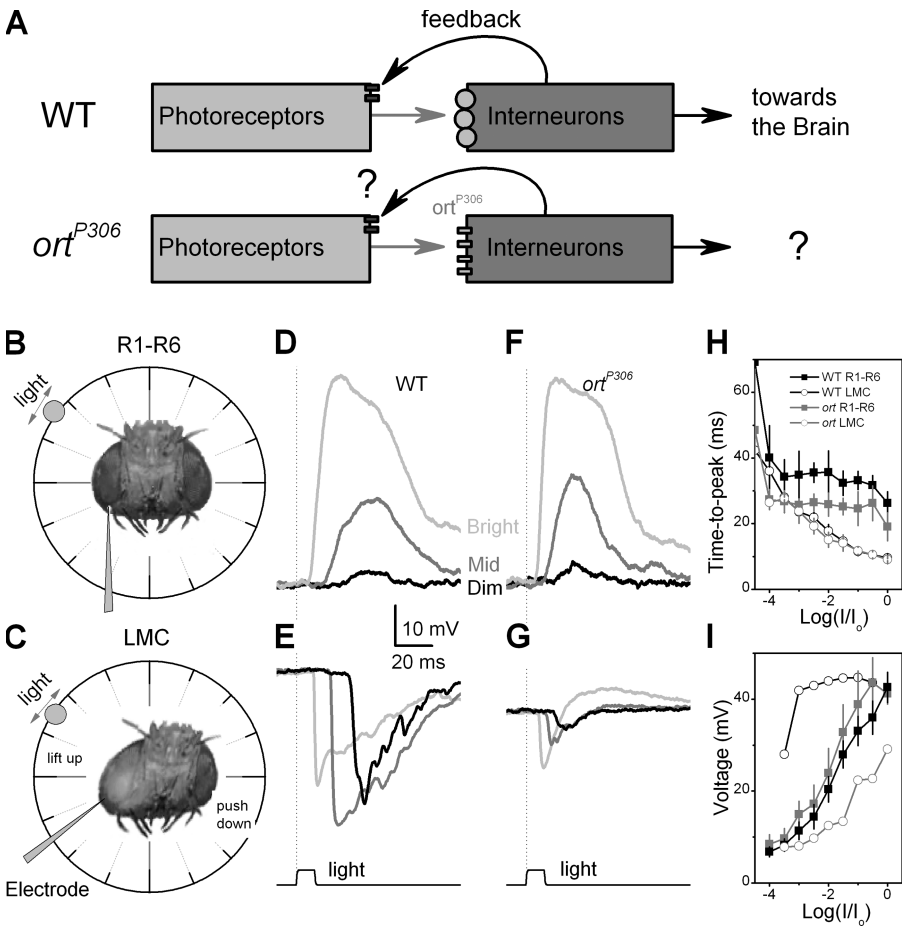

Figure 2. The feedforward and feedback flow of information between photoreceptors and interneurons and pre- and postsynaptic responses in vivo. (A) The simplified wiring diagram of the first visual synapses. The histaminergic output from photoreceptors to the postsynaptic receptors is in red, whereas the synaptic feedback from interneurones to photoreceptor terminal is shown in purple. Electrode approach to (B) R1–R6 photoreceptors and (C) LMCs is different as the recordings from photoreceptor somata were done in retina and the recordings from LMCs were done in lamina. Responses to light pulses from a: (D) WT photoreceptor, (E) WT LMC, (F) ort^{P306} photoreceptor, and (G) ort^{P306} LMC. (H) Time-to-peak of responses at different intensities (WT: R1–R6 photoreceptors, $n = 5$; LMCs, $n = 5$; ort^{P306}: R1–R6 photoreceptors, $n = 6$; LMCs, $n = 5$). (I) Maximum voltage responses of cells to naturalistic stimulation of different intensities (given as absolute values; WT and ort^{P306} R1–R6 $n = 7$; representative LMC series). Mean ± SD shown. Light pulses lasted 10 ms, with the shown intensities having on average 18.5 (dim), 6,000 (mid), and 18,500 (bright) photons.

To scrutinize the findings of intracellular recordings, we further recorded the eye's electrical responses to light pulses, so-called ERGs, by placing surface electrodes on WT flies and ort^{P306} mutants. Fig. 3 A shows that ERGs of WT flies have prominent on- and off-transients superimposed on a slower background signal, whereas Fig. 3 B shows that in ort^{P306} ERGs, these transients were much smaller but superimposed on a larger background. The size of the transients is believed to reflect the strength of signal transfer from photoreceptors to primary visual neurons, with the slower background signals being generally attributed to more graded responses of photoreceptors. However, owing to the lack of intracellular recordings, these assumptions have never been tested in *Drosophila*. Our data shows that at least for ort^{P306} this correspondence is clear. The differences between their ERG transients and those of WT flies (on-transients, Fig. 3 C; off-transients, Fig. 3 D) agree with the voltage responses of their LMCs, which are similarly smaller (compare Fig. 2, E and G, light gray traces). Furthermore, the respective waveforms of the background signals are systematically faster and larger in ort^{P306} (Fig. 3, A, B, and E), correlating well with the intracellularly measured photoreceptor outputs (compare Fig. 2 I).

Judged by the size and speed of responses in ort^{P306} LMCs, the first visual synapses function reasonably well under bright illumination. To test whether this level of transmission is sufficient for carrying visual information to the brain, and for seeing, we compared phototaxic behavior of ort^{P306} mutants to that of WT flies, using a simple paradigm where walking flies have to choose between light and dark surroundings (Fig. S2). These experiments showed that both ort^{P306} mutants and WT flies exhibit strong phototaxis toward bright light, with no significant differences between these groups.

We summarize the findings from ort^{P306} mutants. Both intracellular and ERG recordings and behavioral experiments indicate that under bright illumination a significant amount of visual information can be transmitted across malfunctioning histaminergic receptors to the primary visual interneurones and further to the brain, and that this is associated with enhanced photoreceptor output. These findings are consistent with, but cannot yet substantiate, the hypothesis of photoreceptor output being modulated by synaptic feedback from the interneurons.

Evidence that Synaptic Feedback Modulates Photoreceptor Output

Besides feedback from the interneuron network, there are at least two other plausible mechanisms that could enhance the responsiveness of ort^{P306} photoreceptors.

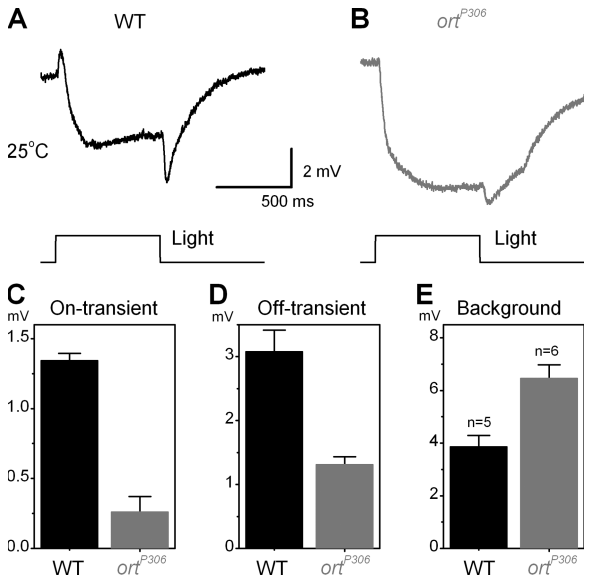

Figure 3. Typical WT (A) and *ort*^{P306} ERGs (B) to a bright light pulse. While ERGs of WT flies show prominent on- (C) and (D) off-transients, the transients in *ort*^{P306} ERGs are much smaller. The data agrees well with the smaller voltage responses of *ort*^{P306} LMCs (compare Fig. 2, E and G). Furthermore, the size of the background response (E), generally attributed to the voltage responses of photoreceptors, are larger and rising faster in *ort*^{P306} ERGs, corresponding to the larger and faster voltage responses of *ort*^{P306} photoreceptors (compare Fig. 2 I). (C–E) Mean ± SD shown.

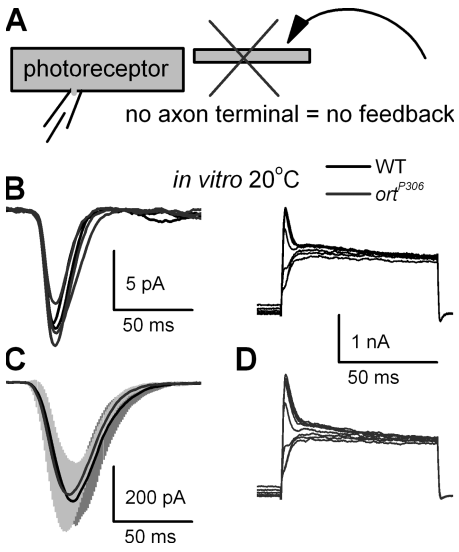

Figure 4. Differences in responses of WT and *ort*^{P306} photoreceptors are not caused by phototransduction or modified K^+ conductances. (A) Whole-cell recordings are made in vitro from dissociated photoreceptors that lack axon terminals and therefore receive no synaptic feedback. (B) Responses to single photons (WT traces in black, *ort*^{P306} traces in dark gray; the same coloring in C and D). (C) Mean and SD of responses to light impulses (30,000 photons; SD: WT gray; $n = 3$, *ort*^{P306} light gray; $n = 3$), and (D) outward currents to voltage steps show no significant differences (see also Table S1). The light impulse lasted 1 ms (A and B). All recordings were done at 20°C.

First, it could be caused by additional mutations; second, by homeostatic changes that affect the phototransduction machinery or voltage-gated membrane conductances. To test these hypotheses we examined light- and voltage-gated conductances of WT and *ort*^{P306} photoreceptors in vitro (Fig. 4) using whole-cell recordings from R1–R6 photoreceptors in dissociated ommatidia (Hardie, 1991b) (Fig. 4 A). This procedure, which for technical reasons must be done on young flies within a few hours of post-eclosion (see Materials and Methods) (Hardie, 1991b), severs the photoreceptor axons, thus eliminating all synaptic connections of the photoreceptors, including any synaptic feedback. Since whole-cell patch-clamp recordings of the dissociated *ort*^{P306} photoreceptors indicated that their transduction machineries (Hardie, 1991b) (Fig. 4, B and C) and membrane conductances (Hardie, 1991a) (Fig. 4 D) were indistinguishable from WT (Table S1), the enhanced output of *ort*^{P306} photoreceptors in vivo is unlikely to result from additional mutations or developmental homeostatic changes in photoreceptor somata.

Other evidence gave further independent support for the feedback hypothesis. Current-clamp recordings from dark-adapted WT and *ort*^{P306} photoreceptors in vivo (Fig. 5, A and B, respectively) showed that their resting potentials (Fig. 5 C) and membrane impedances (Fig. 5 D), measured from voltage responses to a small hyperpolarizing current step, were similar. This suggested that the total resting conductances, including the ones at the terminal, had not changed in the mutant (Fig. S3).

However, since the in vitro experiments were done on young flies (Fig. 4), it was still possible that maturation could cause homeostatic changes, gradually enhancing the responsiveness of *ort*^{P306} photoreceptors to the level we observe in older flies. To rule out this possibility we performed light-pulse experiments in vivo on young flies within 12 h post-eclosion (Fig. 5 E). Microsurgery in these experiments was demanding. The cornea of young flies is very soft, yet one must cut a small window on the eye for the microelectrode while keeping the damage minimal. The recordings from successful preparations showed that young *ort*^{P306} photoreceptors had similar response dynamics to those of older mutants (compare Fig. 2 F). Hence, we could conclude that the enhanced responsiveness of *ort*^{P306} photoreceptors was already present at young age, and not induced by maturation.

We also recorded from *ebony* mutant (Hotta and Benzer, 1969) flies, whose faulty histamine recycling is believed to significantly reduce transmission from photoreceptors to LMCs (Borycz et al., 2002). The aim of this experiment was similar to *ort*^{P306} experiments, namely to investigate whether the reduced input to the interneurons would boost photoreceptor output. Fig. 5 F shows that voltage responses of *ebony* photoreceptors were virtually identical to those of *ort*^{P306}, and 40% faster than WT

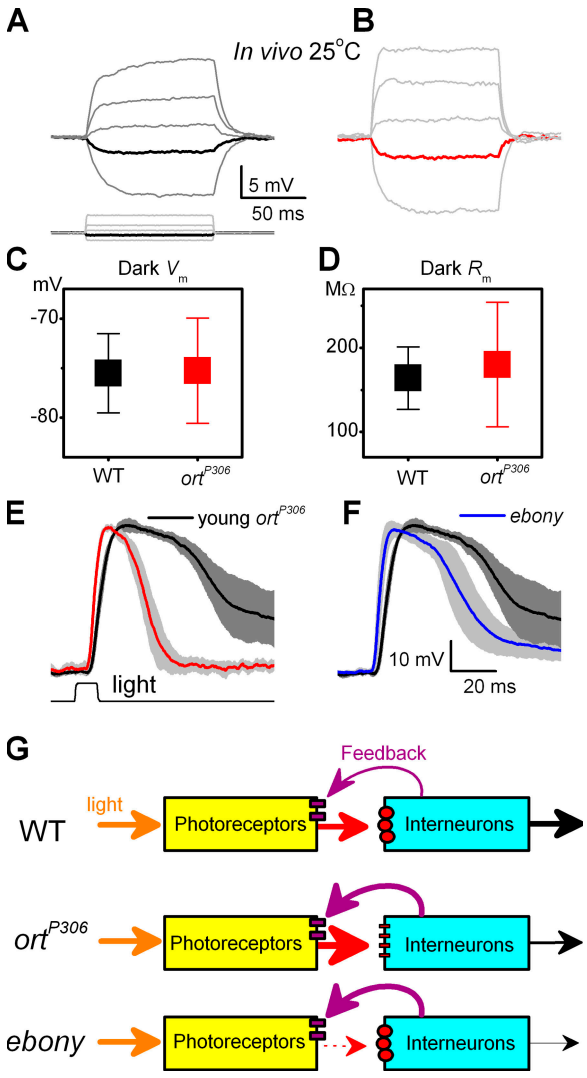

Figure 5. Evidence that the photoreceptor output is modulated by synaptic feedback. Voltage responses of dark-adapted WT (A) and *ort*^{P306} (B) photoreceptors to small hyperpolarizing and depolarizing current pulses in current-clamp recordings in vivo. Responses to a −0.01 nA pulse is shown in black (WT) and in red (*ort*^{P306}) in the respective figures. Notice that the depolarizing voltage responses of *ort*^{P306} photoreceptors are larger and peak earlier than those of WT photoreceptors, similar to our findings with light pulses in Fig. 2. (C) Resting potential of WT and *ort*^{P306} photoreceptors in darkness (mean ± SD, $n = 7$). (D) Impedance of the photoreceptors to −0.01 nA (mean ± SD, $n = 7$). The use of small negative current steps prevents the activation of voltage-gated ion channels (Hardie, 1991a). In both photoreceptors the capacitive voltage charge dies out before the end of the step, at which point the voltage is read and the impedance calculated. Responses of (E) a young *ort*^{P306} ($n = 4$, red, normalized), (F) adult *ebony* ($n = 5$, blue), and WT photoreceptors ($n = 5$, black) to a bright pulse. Mean ± SD shown. *ebony* mutant has a greatly reduced histamine recycling (Borycz et al., 2002), reducing the probability of successful synaptic transmission from photoreceptors to the primary visual interneurons. (G) Graphical representation of the experimental findings. Photoreceptor output is boosted when the histamine receptors (small red circles) on the interneurones malfunction (*ort*^{P306}) or when there is a reduction in histamine release (dotted arrow) from the photoreceptor terminals (*ebony*). Both conditions can be explained by enhanced synaptic feedback from interneurones (thick purple arrows) to photoreceptors.

responses. Hence, the findings from *ort*^{P306} and *ebony* endorse the hypothesis that when the transmission from photoreceptors to interneurons is compromised, the signals that visual interneurones feed back to photoreceptor terminals boost the photoreceptor output (Fig. 5 G).

shibire^{TS1} Shows that Synaptic Feedback Comes via Excitatory Conductances

At this point we do not know whether the enhanced photoreceptor output of the mutants in vivo results from a reduction in inhibitory conductances or from an increase in excitatory conductances to photoreceptor terminals. To resolve this we asked what would happen to the photoreceptor output in vivo if the synaptic feedback ceased? If we expect constant feedback conductances even in darkness, and these are inhibitory, then lack of them would depolarize photoreceptors. Whereas, if the feedback uses excitatory conductances, their silence would hyperpolarize photoreceptors.

We tested this by using a temperature-sensitive synaptic mutant (Poodry et al., 1973; Kawasaki et al., 2000), *shibire*^{TS1}. Warming these mutants to >27°C should silence all their vesicle-driven synaptic transmission. We first verified this for the photoreceptor-LMC synapses by recording intracellularly voltage responses of postsynaptic LMCs to light in *shibire*^{TS1} mutants; synaptic transmission from R1–R6 photoreceptors to LMCs appears normal at low room temperatures, but ceases by warming (Fig. 6, A and B, respectively; Fig. S4). Similarly, warming these mutants should also silence the feedback from the interneurons to photoreceptor terminals. Hence, intracellular recordings from WT and *shibire*^{TS1} photoreceptors, while warming and cooling the flies, should then reveal how the feedback modulates the photoreceptor output (Fig. 6 C, diagram).

Fig. 6, C and D, compares the voltage responses of WT and *shibire*^{TS1} photoreceptors, respectively, to a brief saturating light pulse at 18°C and 28°C. At the cooler temperature, the responses of WT and *shibire*^{TS1} photoreceptors were virtually identical (compare *shibire*^{TS1}, thick blue trace, to WT, dotted blue trace, in Fig. 6 B). In contrast, warming resulted in 10–15 mV hyperpolarization of *shibire*^{TS1} photoreceptors below the resting potential of WT photoreceptors, presumably due to cessation of synaptic feedback to *shibire*^{TS1} photoreceptors (Fig. 6 E; Fig. S5, A–D). Although warming accelerated the voltage responses of both the photoreceptors (the red traces in Fig. 6, C and D), the responses of *shibire*^{TS1} cells had marginally slower rising phases but terminated significantly more quickly (Fig. S5, I–J). These differences could not be explained by heat-induced differences in

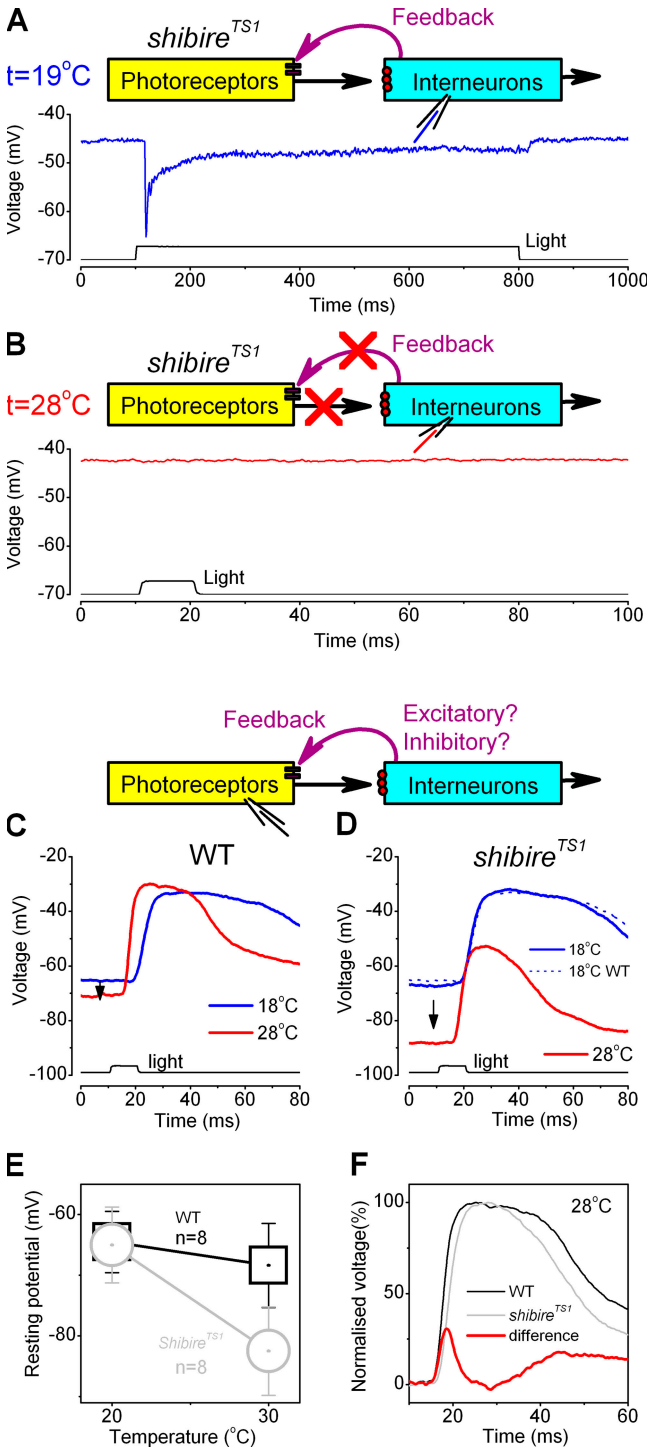

Figure 6. The synaptic feedback to photoreceptor terminals is excitatory and fast, suggesting monosynaptic pathways. Voltage responses of a *shibire*^{TS1} LMC to light pulses (A) at 19°C and (B) at 28°C. At the lower temperature, synaptic transmission is normal, at temperatures >27°C the transmission stops (Chen and Stark, 1990). (C) Voltage responses of a WT photoreceptor to a saturating light pulse at 18°C (blue trace) and 28°C (red trace) in vivo. (D) Voltage responses of a *shibire*^{TS1} photoreceptor to a saturating light pulse at 18°C (thick blue trace) and 28°C (red trace) in vivo. The corresponding mean WT response at 18°C is shown as a dotted blue line. In C and D, each trace is the average of three successive responses. The arrows indicate the warming-induced drop in the resting potentials of the cells. (E) The mean and SD of this hyperpolarization in WT (black squares) and in *shibire*^{TS1} photoreceptors (n = 8). (F) The dynamics of the feedback component (red trace), as the difference between the voltage responses of WT (black) and *shibire*^{TS1} (light gray) photoreceptors at 28°C; data from C and D, respectively. The feedback boosts the rising and decaying phases of the voltage responses to light.

the transduction machineries as the sensitivity of the photoreceptors remained similar and unchanged (Fig. S5 E). Therefore, since there was no synaptic transmission in *shibire*^{TS1} mutants at 28°C, the more depolarized resting potential and faster voltage responses of WT photoreceptors result at least partly from excitatory feedback to WT photoreceptor terminals. Fig. 6 F shows the normalized voltage responses of WT (black) and *shibire*^{TS1} (light gray) photoreceptors to a saturating light pulse at 28°C. The difference of these saturated responses, shown in red, can be used to approximate the waveform of the feedback response when the membrane impedances of the cells are similar (Fig. S5, G–H). The time course of this estimate shows very little delay and resembles that of an inverted LMC response (compare Fig. 2), enhancing the rising and decaying phases of the photoreceptor output, thus suggesting its direct origin from the primary visual interneurons.

Key Elements of a Feedback Model

The results from the light-pulse experiments suggest a simple feedback model for signal transmission between photoreceptors and interneurones. It is known from the anatomy of single neuro-ommatidia that both LMCs and local AC processes receive input from six photoreceptors, and that these interneurons feed back to photoreceptors (Meinertzhagen and O'Neil, 1991). While LMCs also send information directly to higher visual centers, ACs signal upwards only indirectly (Meinertzhagen and O'Neil, 1991). The feedback model we propose builds on these anatomical connections to provide the simplest explanation for the data. It has three assumptions. (1) ACs and LMCs function similarly in the feedback network of a single cartridge, since they both detect histamine changes from the same photoreceptor output synapses (Fig. 1 B, a); more evidence for this assumption will be given by statistical analyses in the next section, while its merits and weaknesses will be argued in the discussion. (2) The feedback from the interneurons to photoreceptor terminals is fast, voltage dependent, and includes a maintained, tonic component, as suggested by the *shibire*^{TS1} experiment (Fig. 6 E), but also since these feedback synapses have characteristic ribbon structures (Meinertzhagen and O'Neil, 1991; Meinertzhagen and Sorra, 2001) typically associated with a high rate of vesicle release (Uusitalo et al., 1995; Juusola et al., 1996). (3) The feedback uses transmitter(s) that activate

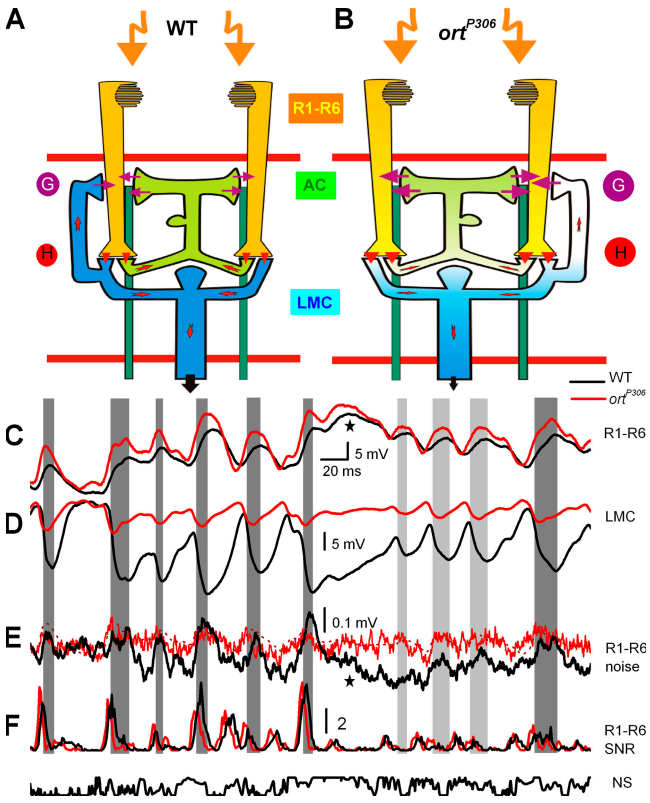

Figure 7. Conceptual feedback model of synaptic transmission within a neuro-ommatidium highlighting the dominant synaptic connections and neural signaling during NS. Feedback from interneurons (AC, green; LMC, blue) to photoreceptors (R1–R6, yellow) in (A) WT and (B) *ort*^{P306}. Interneurons connect with all six photoreceptors; for clarity only R1 and R2 photoreceptors are shown. Arrows indicate the flow of information. The whiter the cells the more depolarized they are. Transmitters: G, glutamate (Sinakevitch and Strausfeld, 2004); H, histamine (Hardie, 1989a). Response properties of photoreceptors and LMCs: WT (black), *ort*^{P306} (red). Cells were dark adapted for 30 s before stimulation. Typical in vivo signals (average responses to 30–150 stimulus sweeps) of (C) photoreceptors, (D) LMCs, and (E) photoreceptor noise SD (mean of four cells) and (F) SNR(*t*)s to bright NS. In E, the dotted line compares noise SD of *ort*^{P306} photoreceptors to a rescaled and inverted voltage trace of an *ort*^{P306} LMC (from D). Gray bars indicate moments in responses of WT LMC from their highest rate of change to troughing.

depolarizing conductances on photoreceptor terminals (Fig. 6, C–E); possibly glutamatergic, as both LMCs and ACs show glutamate-like immunoreactivity (Sinakevitch and Strausfeld, 2004), and/or cholinergic, as suggested by pharmacology (Hardie, 1989b) and immunohistochemistry (Yasuyama et al., 1996). In functional terms, an active feedback should add an extra depolarizing and accelerating component to the voltage response of a photoreceptor (compare Fig. 6 F; Fig. S5 J). When light depolarizes a photoreceptor, LMCs hyperpolarize, because of the sign inversion at the first (histaminergic) synapses. As the voltage drops in LMCs so does their synaptic transmission. This should reduce their feedback component to photoreceptor axon terminals, thereby shrinking and slowing down the photoreceptor output.

Function of the Feedback: (1) Rapid Gain Control

We tested the feedback model in vivo by comparing voltage responses of WT and *ort*^{P306} photoreceptors and LMCs to a 1-s-long bright NS pattern that was repeated 25–150 times (see Materials and Methods). The reason for using *ort*^{P306} for the functional analysis, instead of *shibire*^{TS1}, is that the experiments can be done at a lower temperature (25°C) where long-lasting intracellular recordings are stable and much easier to do, as the flies are less active. To help visualize the function of the feedback, the data is presented with conceptual circuit diagrams, which show the major synaptic connections and the flow of information within a single WT and *ort*^{P306} neuro-ommatidium (Fig. 7, A and B, respectively). Light signals (orange arrows) are processed by photoreceptors (yellow) and transmitted via histaminergic synapses (H) to LMCs (blue) and ACs (light green). These feed back to photoreceptor terminals synaptically via ligand-gated conductances (G). Arrows indicate the magnitude and direction of information flow, while whiteness of circuitry marks increased depolarization.

A 420-ms snapshot shows the mean responses of a photoreceptor and an LMC (Fig. 7, C and D, respectively) from WT flies (black traces) and *ort*^{P306} mutants (red traces). The feedback model predicts that *ort*^{P306} photoreceptors should be affected in the following way. The reduced histamine affinity of LMCs and the AC should make their responses to naturalistic stimulation smaller and faster (see below). Therefore, their responses would have a much reduced operational voltage range and be on average more depolarized than those of WT interneurons (whitened *ort*^{P306} LMC and AC; cf. Fig. 7, A and B), as seen in the data (Fig. 7 D). The more depolarized the interneurons, the more sensitized (dark adapted, operating with a high gain; Juusola et al., 1995) they are, and the more transmitter they release onto photoreceptor terminals, causing an increase in excitatory conductance. Consequently, the feedback in *ort*^{P306} mutants should be stronger, as seen by the larger and faster responses of *ort*^{P306} photoreceptors in Fig. 7 C (whitened axons of *ort*^{P306} photoreceptors; cf. Fig. 7, A and B). In this way, the interneuron feedback provides gain control for the first visual synapses. When the probability of saturating LMCs is low (Fig. 7 D, red line), feedback to photoreceptor terminals is strong (Fig. 7 C, red line). When responses of LMCs become large (Fig. 7 D, black line), feedback reduces (Fig. 7 C, black line). The responses of *ort*^{P306} photoreceptors are faster for two reasons (Fig. 7 C and Fig. 2 H). The enhanced synaptic feedback increases their membrane conductances, thus giving them a smaller membrane time constant (Fig. 7 C; cf. responses to depolarizing current steps in Fig. 4, A and B).

The second factor is that the feedback signals themselves are briefer (Fig. 7 D), attributable, at least partly, to the faster dynamics of histamine-gated ort^{P306} receptors on the LMC membrane (Fig. 2 G).

Function of the Feedback: (2) Regulation of the Signal Quality

The second prediction of the feedback model concerns network noise. The small size and high membrane impedance of *Drosophila* photoreceptors provide favorable electrophysiological conditions where the effects of synaptic feedback, although weakened by the distance, can still be detected when recording from their somata (Juusola and Hardie, 2001a). This should be seen as extra noise coming from the many synapses of the feedback network at particular points in time. The main origin of the noise is in the ligand-gated receptors, either histaminergic on the interneurons or probably glutamatergic and/or cholinergic on the photoreceptors (Hardie, 1989b; Yasuyama et al., 1996; Sinakevitch and Strausfeld, 2004). We expect lower noise when most of the receptor-bound ion channels on photoreceptors are open, i.e., when sufficiently high transmitter levels are being released from interneurons. Therefore, the noise variance (see Materials and Methods) in photoreceptor responses should peak when the interneurons are the most hyperpolarized. Fig. 7 E shows the mean noise variance of four WT photoreceptors, chosen from experiments where naturalistic stimulation was repeated >100 times. The dynamics of noise variance mirror the LMC potential with clear peaks appearing when LMCs hyperpolarize the most, as predicted by the feedback model. Since the noise variance peaks when noise from light- and voltage-gated channels in photoreceptors is minimum (Hardie, 1991a; Juusola and Hardie, 2001a) and it decays (Fig. 7 E, star) when the responses, and thus noise in the photon arrival, is the largest (Fig. 7 C, star), presynaptic explanations can be ruled out (see Fig. S1, A and B). In *ort^{P306}* mutants, the model predicts that, owing to the smaller amplitude and briefer transients in the responses of LMCs, the mean noise variance of their photoreceptors should show smaller and briefer peaks. This is also evident in Fig. 7 E.

What is the effect of the feedback on the information transfer? Because LMCs sum the input from six photoreceptors that receive visual input from the same visual field (Kirschfeld, 1967), their SNR is higher than that of a single photoreceptor (Srinivasan et al., 1982; Laughlin et al., 1987; van Hateren, 1992; Juusola et al., 1995; de Ruyter van Steveninck and Laughlin, 1996; van Hateren and Snippe, 2001). Likewise, we expect the same principle working for local ACs. By sharing each tetrad synapse with two LMCs, amacrine cells receive similar input from R1–R6 photoreceptors as the monopolar cells. Therefore, SNR of ACs should be similarly enhanced as that of LMCs. To study whether the feedback from LMCs and ACs improves presynaptic signaling we compared the dynamics of the SNR in WT and *ort^{P306}* photoreceptors. Given that hyperpolarization of LMCs and ACs reduces the feedback, most peaks on the WT photoreceptor SNR occur during their responses to transient light changes (Juusola and de Polavieja, 2003) (Fig. 7 F, black line). In *ort^{P306}* mutants, since their interneurons are more depolarized and their responses are richer in high frequencies (Fig. 7 D; red and black lines, respectively), the enhanced feedback typically makes the SNR of their photoreceptors reach higher values with faster rising and briefer peaks (Fig. 7 F, red line).

Additionally, we assess the effect of feedback on information transfer in WT and *ort^{P306}* photoreceptors and LMCs at different luminances (Fig. 8, A and B; see Materials and Methods). The extra high frequency feedback of high SNR from the interneurons should boost the SNR of *ort^{P306}* photoreceptors. This is indeed what we observe (Fig. 8 A, red and black lines, respectively) at all but the dim stimulation, where the photon shot noise dominates. The SNR of *ort^{P306}* LMCs is well below that of WT LMCs at dim stimulation and at low frequencies (Fig. 8 B, red and black lines, respectively). Yet, at bright stimulation, the SNR of *ort^{P306}* LMCs is above that of WT LMCs at medium and high frequencies. These results were further quantified by calculating the corresponding information transfer rates (R). Fig. 8 C shows that brightening, i.e., increasing the stimulus SNR, generates a concomitant increase in information transfer rates of photoreceptors and LMCs. Since the observed enhanced responsiveness in *ort^{P306}* photoreceptors originates from the enhanced feedback of high SNR, they can carry more information than the WT photoreceptors across the luminance levels. This allows the throughput of *ort^{P306}* LMCs to reach the values of WT LMCs at bright stimulation.

DISCUSSION

In this study we have presented compelling evidence that synaptic feedback from the primary visual interneurones modulate the photoreceptor output in *Drosophila* compound eye. We have shown that the feedback circuitry improves information processing, providing a high throughput for rapid changes in the natural environment and proposed the simplest negative feedback model that can explain these findings. In the following paragraphs we compare our model to other possible models, before closing on general comments about the use of feedback synapses in sensory systems.

Model of Synaptic Signal Transfer from Photoreceptors to the Primary Visual Interneurons

Results from *ort^{P306}*, *ebony*, and *shibire^{TS1}* photoreceptors (Fig. 6) and noise analysis of WT photoreceptors

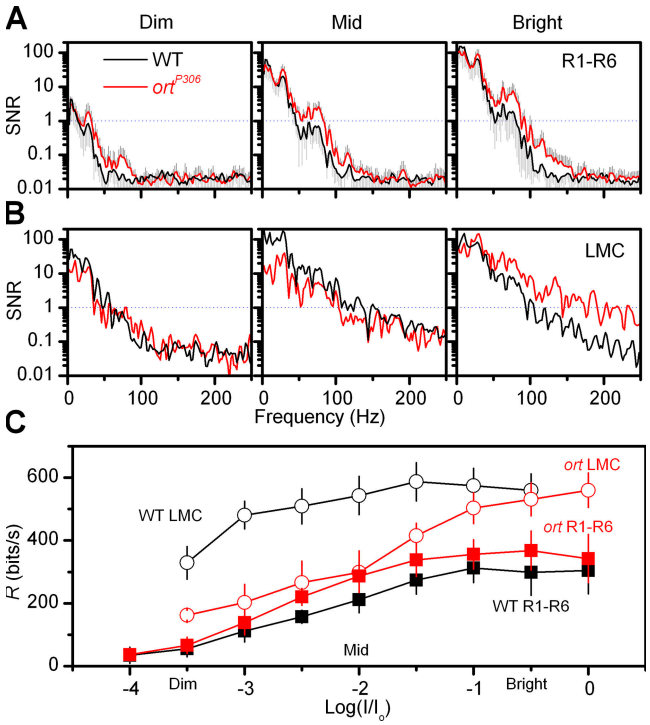

Figure 8. SNR(f) and information transfer rate, R, in WT (black) and ort^{P306} (red) photoreceptors and LMCs across a 4-log range of intensities. SNR(f) of (A) photoreceptors (n = 7) and (B) LMCs (n = 3) to dim (left), middle, and bright (right) naturalistic stimulation. (C) Information transfer rate, R of cells. ort^{P306} photoreceptors outperform WT (n = 7). Summing input from six photoreceptors, WT LMCs (n = 3) convey six times more information than a photoreceptor at dim naturalistic stimulation, but only two times at bright stimulation as the channel capacity approaches its limit. In ort^{P306}, this ratio is typically less than 3:2, but at bright stimulation the enhanced signals of photoreceptors help ort^{P306} LMCs reach equally high information transfer rates as WT LMCs. Mean ± SD shown.

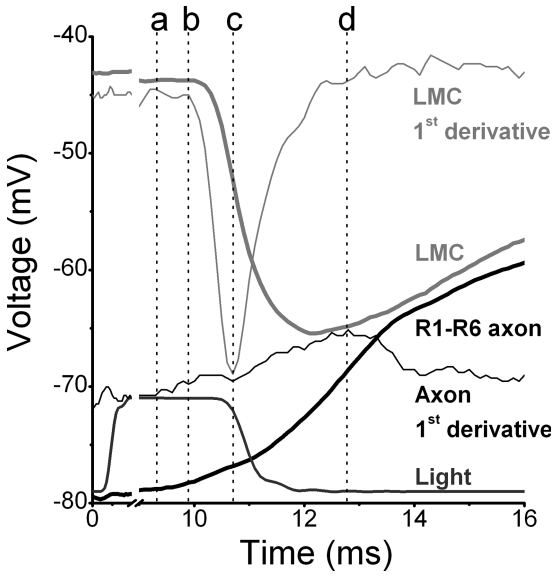

Figure 9. Comparison of pre- and postsynaptic waveforms, recorded from lamina of WT flies at 25°C. High-quality voltage responses of an R1–R6 photoreceptor axon (black thick trace) and an LMC (light gray thick trace) and their corresponding first derivatives (thin traces of respective colors) to a 10-ms bright light pulse (18,500 photons; dark gray trace). Notice the x-axis break. The photoreceptor begins to depolarize 9 ms after the light onset (marked by dotted line at a) followed by initiation of a transient hyperpolarization in the LMC (b). When the rate of LMC hyperpolarization is at its fastest (c), the rate of photoreceptor depolarization reaches its local minimum. The photoreceptor depolarizes at its fastest rate (d) soon after LMC has begun to depolarize.

(Fig. 7 E) strongly suggest that a simple negative feedback loop, combining sign-inverting graded potential synapses with a feedback circuitry of excitatory transmitters (Yasuyama et al., 1996; Sinakevitch and Strausfeld, 2004), regulates signal transfer from photoreceptors to LMCs. This overall framework can be further supported by directly comparing pre- and postsynaptic voltage responses on a stretched time scale, making it possible to roughly work out some time-dependent properties of this coding.

Fig. 9 illustrates typical correlations in high-quality (low noise) voltage responses of a WT photoreceptor axon (recorded in lamina; black thick line) and a WT LMC (gray thick line), and their rates of change (thin lines), to a 10-ms-long bright pulse (thin dark gray line). Phototransduction mechanisms have an absolute time delay (Juusola and Hardie, 2001a), so only ~9 ms after the stimulus onset the photoreceptor axon begins to depolarize (a). As the photoreceptor depolarizes, its histamine release increases, and the LMC hyperpolarizes (b). This leads to a transient reduction in the excitatory feedback to the photoreceptor axon terminal (c), i.e., reduction of the transmitter release from the interneurons, slowing down the rate the photoreceptor is depolarizing (c). As soon as the rate of hyperpolarization in the LMC begins to decelerate, the boost from the feedback to photoreceptor terminals picks up again. It reaches its maximum, seen as the fastest rise in the photoreceptor depolarization (d), moments after the LMC begins to depolarize.

The fast action of the feedback on photoreceptor output (Fig. 9, Fig. 6 D, and Fig. 7 E) suggests that it comes from the direct synaptic connections of LMCs and ACs to photoreceptor terminals. To follow rapid changes in light input, the feedback requires tonic transmitter release. This notion is supported by ultrastructural studies. The fact that the output and feedback synapses in photoreceptor axon terminals occupy neighboring microdomains with minimal diffusional constraints and substantial vesicle pools (Meinertzhagen and O'Neil, 1991; Meinertzhagen and Sorra, 2001) should make the feedback nearly instantaneous and thus able to prevent the postsynaptic histamine receptors from saturation. In this respect, the automatic balancing of synaptic drives resembles predictive coding, usually associated with neural inhibition (Srinivasan et al., 1982).

There are four reasons why we believe that our assumption of sign inverting amacrine cells, which hyperpolarize to light increments, is likely to be correct. First, since amacrine cells contribute the majority of the synapses (~65%) to photoreceptor axon terminals (Meinertzhagen and Sorra, 2001), we expect that the waveforms (Fig. 6 F) feeding back to photoreceptors to be dominated by the dynamics of this circuit. Second, over the years there has been a considerable research effort for recording electrical responses from lamina of dipteran flies (Järvilehto and Zettler, 1971; Srinivasan et al., 1982; Laughlin et al., 1987; Hardie et al., 1988, 1989a,b; Srinivasan et al., 1990; James, 1992; van Hateren, 1992; Juusola et al., 1995; Uusitalo et al., 1995; de Ruyter van Steveninck and Laughlin, 1996; van Hateren, 1997; van Hateren and Snippe, 2001), yet these studies have provided no compelling evidence for graded depolarizing responses beyond those attributed to photoreceptor axons and slower laminal field potentials. Since the web of amacrine cells in lamina is dense, some of the hyperpolarizing responses should have come from amacrine cells (see also Shaw, 1984). Third, our data shows that the synaptic feedback enhances the information transfer rate of photoreceptors (Fig. 8 C), and that the noise characteristics of photoreceptors mirror the response dynamics of LMCs (Fig. 7 E). These findings strongly suggest that the separate feedback circuits from LMCs and ACs to photoreceptors are synchronized and in the same phase. Fourth, at temperatures >27°C all synaptic transmission in *shibire^{TS1}* mutants ceases (Figs. S4 and S5; Chen and Stark, 1993; *Shibire^{TS}* has been very widely used and found to block synaptic transmission at all synapses investigated, both graded and spiking, e.g., van der Bliek and Meyerowitz, 1991; Kitamoto, 2001). Naturally, this should include both amacrine cell and LMC feedbacks. In such conditions, the total waveform of the signals fed back to photoreceptors can be approximated as the difference between the voltage responses of WT and *shibire^{TS1}* photoreceptors, given that the light stimulus is the same and the membrane impedances of the photoreceptors are similar. Since this total signal from the primary visual interneurones resembles the inverted voltage response of LMC (Fig. 6 F and Fig. S5 J), it is probable that its amacrine cell and LMC components are similar.

However, a recent publication by Douglass and Strausfeld (2005) apparently challenges this view. They report obtaining intracellular recordings from three amacrine cells in *Phaenicia* and show partially dye-filled processes of these neurons as evidence. The responses to light increments are small depolarizations (<5 mV), which according to their frequency responses are slower and more delayed than those of photoreceptors. Hence, judged by their waveforms, these responses could not be the main components of the fast synaptic feedback we have presented in this paper. However, if the recorded responses showed the total output of amacrine cells, then the synthesis would be that, regardless of their dominating prevalence, amacrine cell synapses are providing a weaker, tonic feedback to photoreceptor axon terminals, whereas the larger and faster responses from monopolar cells (L2 and possibly L4) would provide the dynamic modulation. To further investigate this we have started producing transgenic flies that ultimately should elucidate the role of different feedback synapses in lamina.

Comparison to Other Models

Other models have inconsistencies with the data. Here we compare our findings to three models, each based on different premises: inhibitory conductances, histaminergic autoreceptors, and homeostatic increase in histamine release.

We start by imagining a model whereupon a negative feedback from primary visual interneurones to photoreceptors uses inhibitory conductances. According to such a model, the responses of WT photoreceptors are smaller and slower because the feedback from the interneurons reduces their size and speed, while responses of *ort^{P306}* photoreceptors are larger and faster because this feedback is silent. However, this explanation is contradicted by the results from (1) *shibire^{TS1}* (Fig. 6), which establishes that the conductances involved are excitatory and have a tonic component. Further experimental evidence for this are: (2) WT and *ort^{P306}* photoreceptors have similar resting potentials (Fig. 5 C) and (3) membrane impedances (Fig. 5 D). In addition, (4) the signaling performances of *ort^{P306}* photoreceptors are better than those of WT photoreceptors (Fig. 8, A and C), requiring an increased, not reduced, flow of information from visual interneurons.

Could histaminergic autoreceptors explain the enhanced photoreceptor output? Autoreceptors, although never shown in *Drosophila* photoreceptors, have been speculated to form a negative feedback (Hardie et al., 1988) that regulates the level of histamine release from photoreceptor terminals. As such they should hyperpolarize, owing to chloride conductance, to light, otherwise the feedback would be positive, leading to a rapid increase in histamine concentration and saturation of the post-synaptic receptors. Several factors make it unlikely that histaminergic autoreceptors are responsible for the enhanced output of *ort^{P306}* photoreceptors. Comparison between in vitro (Gengs et al., 2002) and in vivo data from *ort^{P306}* LMCs (Fig. 2 F) suggests that histamine release from photoreceptors is increased. Hence, if autoreceptors were functional in *ort^{P306}* mutants, they would hyperpolarize photoreceptors more than those of WT flies. On the other hand, if they were sub- or nonfunctional, the *ort^{P306}* photoreceptors would depolarize more than WT photoreceptors. Our data

contradicts these statements by showing that (1) the resting potentials of ort^{P306} and WT photoreceptors are similar, and that (2) $shibire^{TS1}$ photoreceptors hyperpolarize when the synaptic transmission, and so also the histamine binding to possible autoreceptors, is silenced by warming (Fig. 6). Therefore, we rule out the hypothesis that hyperpolarizing conductances via histaminergic autoreceptors would be the cause for the enhanced output of ort^{P306} photoreceptors.

Finally, we consider why homeostatic mechanisms increasing histamine release from the photoreceptor terminals alone fail to explain our findings. Light-adaptational augmentation of the voltage responses in ort^{P306} LMCs could not only stem from the activity of enhanced synaptic feedbacks but also from a homeostatic increase in the histamine release from the photoreceptor terminals. However, our data do not support the latter mechanism alone, as this would increase the presynaptic noise, or at best keep it unchanged. The fact that the SNR of ort^{P306} photoreceptors is higher than that of the WT photoreceptors means that extra information must be channeled to ort^{P306} photoreceptors from a source that has a higher SNR than that of a single photoreceptor. As the phototransduction machineries and membrane properties, i.e., the capture and processing of light signals, are identical in WT and ort^{P306} photoreceptors, this extra information can only arrive from the feedback network, which, attributable to signal pooling (neural superposition), is the only local neural component (source) having a higher SNR than that of a single photoreceptor.

Dissecting the Feedback Model

We now examine how feedback shapes voltage responses of photoreceptors by schematically comparing the effects of different components of the feedback (Fig. 10). We start by dividing the voltage responses of a photoreceptor into two components: the phototransduction response and the excitatory feedback from interneurons. To keep the comparisons simple we consider a 45-mV phototransduction response to a light flash and a 10-mV feedback background (Fig. 6 C). Notice that while in reality the underlying conductances add and subtract, not the resulting voltages, this approximation can be safely used for stressing the major differences in the responses of wild-type and mutant photoreceptors, since the membrane impedances of these cells were similar (Fig. 5 D; Fig. S5). The resting potential of photoreceptors in darkness without the feedback is −85 mV (Fig. 6 D). Apart from the fairly uncertain transmission gain characteristics of the feedback synapses (but see Fig. 6 F and Fig. 7 E), this generalization gives us four cases to consider, labeled from a to d (Fig. 10 A).

In the first case (a), photoreceptors have no feedback. Phototransduction alone generates a 45-mV response superimposed on a −85 mV resting potential, i.e., the response peaks around −40 mV. The lack of feedback conductances makes the membrane time constant large and so the rise of the response to a light flash relatively slow. On the other hand, the lack of depolarizing feedback conductances makes the decay of the response fast, and thus the total response duration relatively brief. This condition arises when warming $shibire^{TS1}$ (Fig. 6 D) and when the photoreceptors are dissociated in vitro.

In the second case (b), a static feedback background gives a resting potential of −75mV. The phototransduction response occurs in the absence of dynamic feedback, giving a 45-mV response and depolarization to −30 mV. The feedback conductances keep the membrane time constant small, making the rise of the response to the light flash faster than without the feedback (a) (Fig. 10 A). As the feedback signal has no dynamic component, the maximum amplitude (Fig. 10 B) and the decay of the voltage response (Fig. 10 B) are similar to case a, hence the total duration of the response is slightly briefer than without the feedback (Fig. 10 C).

The third case (c) describes the wild-type (WT) condition. Background feedback causes a −75-mV resting potential. The phototransduction response begins to depolarize the cell. Dynamic feedback, which rapidly reduces as the interneurones hyperpolarize and is nearly turned off as they peak, allows the presynaptic potential to reach −25 mV. This 50-mV response is larger and peaks faster than when there is no feedback (a) (Fig. 10, B and A, respectively). When the phototransduction response decays, the depolarizing feedback conductances gradually increase, prolonging the voltage response, although the membrane time constant of WT photoreceptors is now less than without the feedback conductances (a). Thus, the photoreceptor responses are larger and faster, still outlasting case a; yet, they are larger but slower than in case b (Fig. 10, B and C).

The fourth case (d) describes ort^{P306} mutant photoreceptors. Background feedback gives a −75-mV resting potential. A phototransduction occurring with a reduced dynamic feedback on a tonic background gives us a 53-mV response. Because of the reduced throughput of the histamine-gated receptors (Gengs et al., 2002), the ort^{P306} interneurons spend their time at high depolarizing potentials, normally used for dark adaptation (Juusola et al., 1995). In this state of high gain (Juusola et al., 1995) (compare the response of a WT LMC to a dim pulse, Fig. 2 D), the feedback greatly amplifies fast changes in the photoreceptor output. This also keeps the membrane time constant of photoreceptors constantly small. Thus the voltage responses of photoreceptors are now only slightly larger than in case c, peak faster than in cases a and c, and last longer than cases a and b (Fig. 10, A and B).

Since both the static feedback model (b) and the enhanced feedback model (d) generate relatively similar

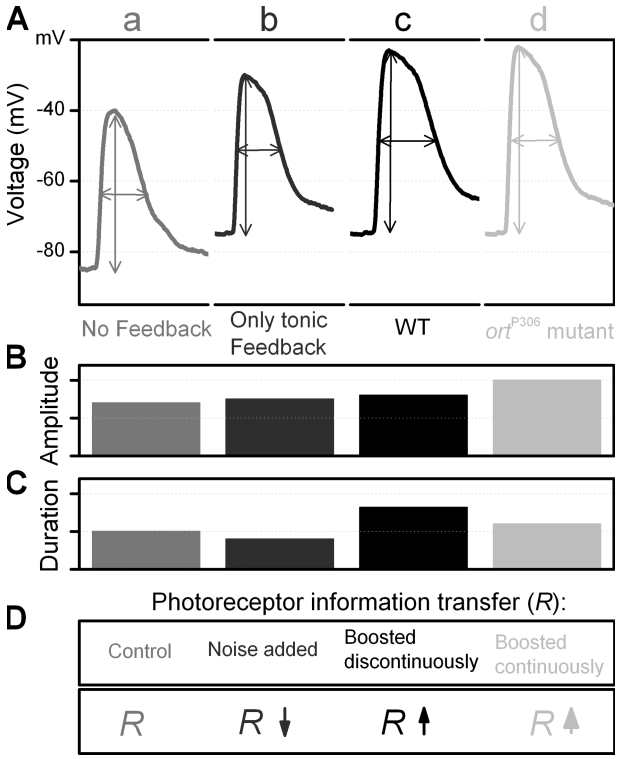

Figure 10. Schematic and qualitative representation of how negative feedback shapes voltage responses of a dark-adapted photoreceptor to a light impulse. (A) Photoreceptor responses: a, when there is no feedback; b, when there is only a static feedback background; c, of WT flies; d, of ort^{P306} mutant. (B) Effect of different feedback conditions on the response size. (C) Effect of different feedback conditions on the response speed. (D) Effect of different feedback conditions on the photoreceptor information transfer rate, *R*.

voltage responses, how can we conclude that the dynamics of ort^{P306} photoreceptors are explained by enhanced feedback (d)? The answer comes from the signaling performances of WT and mutant photoreceptors and LMCs (Fig. 7 and Fig. 8 D). Static feedback (b) can be safely ruled out by two sets of observations. First, the SNR and information transfer rate, *R*, of ort^{P306} photoreceptors are higher than those of WT photoreceptors (Fig. 8, A and C) and second, the signaling performance of ort^{P306} LMCs improves with light adaptation (Fig. 8, B and C). Both of these findings are consistent with our feedback model (d), but against the model (b) where there would be no response in ort^{P306} LMCs and the feedback would increase noise in the photoreceptors, decreasing their SNR and information transfer rate (Fig. 10 D). The dynamic nature of the feedback is further supported by differences in voltage responses of WT and $shibire^{TS1}$ photoreceptors as shown in Fig. 6 F.

A recent paper by Rajaram et al. (2005) reports photoreceptor output being affected by mutations in higher processing centers of *Drosophila*. Although their data (ERG recordings and voltage responses of photoreceptors) cannot provide any mechanism for this phenomenon, they suggest that the photoreceptor function is top-down-regulated. This general concept is in concordance with our findings.

General Coding Considerations

The signals of the interneurons, the LMCs, and the amacrine cells, are enriched by pooling outputs of six photoreceptors looking at the same visual field (Kirschfeld, 1976). The more such signals are fed back to photoreceptors, while keeping within the limits of amplitude and frequency ranges, the better their signaling performance. In our model, the SNR and information transfer rate of WT photoreceptors are reduced in respect to ort^{P306} by silencing the feedback during depolarizations. This effectively cuts off the highest frequencies from their responses, yet prevents saturation of signals at the photoreceptor-LMC synapses. While in ort^{P306} photoreceptors, the feedback is never cut off and thus the phototransduction can be continuously boosted by the high frequency feedback signals of high SNR. Hence, the SNR and information transfer rate of individual ort^{P306} mutant photoreceptors increases over that of WT photoreceptors. Notice, however, that the feedback to WT photoreceptors both accelerates their responses and enhances their SNR over photoreceptors that lack synaptic feedback (Fig. 10, case a). In WT flies, the active feedback network seems to modulate the photoreceptor output such that the synaptic information transfer rate becomes almost independent of the intensity (Fig. 8 C). By doing this, the feedback circuits could ensure that independent of the light intensity of the naturalistic stimulus pattern, the bandwidth of the neural pathway to the brain is used optimally (compare van Hateren, 1992).

Our findings follow the general engineering principles of feedback loops: enhancing reliability, SNR, and bandwidth (Marmarelis and Marmarelis, 1978). Yet, it is the dynamic adaptive nature of the feedback that makes this mechanism different from manmade operational amplifier circuits. As the feedback automatically balances different synaptic drives to ensure a reliable representation of changing sensory inputs, it has a low probability of overloading or causing unwanted oscillations. For this reason alone, it is feasible that analogous designs could be used elsewhere in the nervous systems (Dowling and Chappell, 1972; Burrows and Siegler, 1976; Wässle, 2004; van Kleef et al., 2005). Particularly, we see its usefulness for closed-loop systems that require predictive gain control to match output with the flow of sensory input, or error signals to balance the intended action to the sensory input. In some cases, the known circuitry is already suggestive. For example, in the vertebrate retina, photoreceptors feed information to horizontal cells through glutamatergic excitatory synapses (Wässle, 2004). Here, light hyperpolarizes both

photoreceptors and horizontal cells (Sterling, 1983). Whether the horizontal cells in the vertebrate retina feed their output back to the receptors or to bipolar cells, or to both, varies among species (Kaneko, 1979). The transmission from horizontal cells to photoreceptors and ON-bipolar cells is inhibitory and to OFF-bipolar cell excitatory, as is seen with lateral inhibition (Kaneko, 1979), and thus has the capability to enhance the information processing as we have shown for *Drosophila*.

We thank Cahir O'Kane, Ian Meinertzhagen, Olivier Faivre and Hugh Robinson for comments on the manuscript and Richard Baines (University of Warwick, Coventry, UK), Andrea Brand (Wellcome Trust/Cancer Research UK Gurdon Institute, Cambridge, UK), and Alberto Ferrús (Cajal Institute, Madrid, Spain) for providing us with different mutants. Special thanks to Marta Rivera for assisting with the phototaxis experiments.

This research was supported by grants from BBSRC (M. Juusola and R.C. Hardie), the Royal Society (M. Juusola and G.G. de Polavieja), the Gatsby Charitable Foundation (M. Juusola), MCyT (G.G. de Polavieja), fBBVA (G.G. de Polavieja), CAM-UAM (G.G. de Polavieja), and MRC (R.C. Hardie).

David C. Gadsby served as editor.

Submitted: 12 December 2005
Accepted: 30 March 2006

REFERENCES

Borycz, J., J.A. Borycz, M. Loubani, and I.A. Meinertzhagen. 2002. tan and ebony genes regulate a novel pathway for transmitter metabolism at fly photoreceptor terminals. *J. Neurosci.* 22:10549–10557.

Burrows, M., and M.V. Siegler. 1976. Transmission without spikes between locust interneurones and motoneurones. *Nature.* 262:222–224.

Campos-Ortega, J.A., and N.J. Strausfeld. 1973. Synaptic connections of intrinsic cells and basket arborizations in the external plexiform layer of the fly's eye. *Brain Res.* 59:119–136.

Chen, D.-M., and W.S. Stark. 1990. The effects of temperature on visual receptors in temperature-sensitive paralytic paralytic *shibire* (shits) mutant *Drosophila*. *J. Insect Physiol.* 39:385–392.

de Ruyter van Steveninck, R.R., and S.B. Laughlin. 1996. The rate of information transfer at graded-potential synapses. *Nature.* 379:642-645.

Douglass, J.K., and N.J. Strausfeld. 2005. Sign-conserving amacrine neurons in the fly's external plexiform layer. *Vis. Neurosci.* 22:345–358.

Dowling, J.E., and R.L. Chappell. 1972. Neural organization of the median ocellus of the dragonfly. II. Synaptic structure. *J. Gen. Physiol.* 60:148–165.

Fischbach, K.-F., and A.P.M. Dittrich. 1989. The optic lobe of *Drosophila melanogaster*. I. A Golgi analysis of wild-type structure. *Cell Tissue Res.* 258:441–475.

Gengs, C., H.T. Leung, D.R. Skingsley, M.I. Iovchev, Z. Yin, E.P. Semenov, M.G. Burg, R.C. Hardie, and W.L. Pak. 2002. The target of *Drosophila* photoreceptor synaptic transmission is a histamine-gated chloride channel encoded by ort (hclA). *J. Biol. Chem.* 277:42113–42120.

Götz, K.G. 1964. Optomotoric study of the visual system in some eye mutants of the fruitfly *Drosophila*. *Kybernetik.* 2:77– 92.

Hardie, R., S. Laughlin, and D. Osorio. 1988. Early visual processing in the compound eye: physiology and pharmacology of the retina-lamina projection in the fly. *In* Neurobiology of Sensory Systems. R. Singh and N. Strausfeld, editors. Plenum Press, New York. 23–42.

Hardie, R.C. 1989a. A histamine-activated chloride channel involved in neurotransmission at a photoreceptor synapse. *Nature.* 339:704–706.

Hardie, R.C. 1989b. Neurotransmitters in compound eyes. *In* Facets of Vision. D.G. Stavenga and R.C. Hardie, editors. Springer-Verlag, New York. 235–256.

Hardie, R.C. 1991a. Voltage-sensitive potassium channels in *Drosophila* photoreceptors. *J. Neurosci.* 11:3079–3095.

Hardie, R.C. 1991b. Whole-cell recordings of the light induced current in dissociated *Drosophila* photoreceptors: evidence for feedback by calcium permeating the light-sensitive channels. *Proc. R. Soc. Lond. B. Biol. Sci.* 245:203–210.

Heisenberg, M., and E. Buchner. 1977. The role of retinula cell types in visual behavior of *Drosophila melanogaster*. *J. Comp. Physiol. [A].* 117:163–182.

Hotta, Y., and S. Benzer. 1969. Abnormal electroretinograms in visual mutants of *Drosophila*. *Nature.* 222:354–356.

James, A.C. 1992. Nonlinear operator network models of processing in the fly lamina. *In* Nonlinear Vision: Determination of Neural Receptive Fields, Function, and Networks. R.B. Pinter and B. Nabet, editors. CRC Press, Boca Raton. 39–72.

Järvilehto, M., and F. Zettler. 1971. Localized intracellular potentials from pre- and postsynaptic components in the external plexiform layer in an insect retina. *Z Vergl Physiol.* 75:422–440.

Juusola, M., and G.G. de Polavieja. 2003. The rate of information transfer of naturalistic stimulation by graded potentials. *J. Gen. Physiol.* 122:191–206.

Juusola, M., A.S. French, R.O. Uusitalo, and M. Weckström. 1996. Information processing by graded-potential transmission through tonically active synapses. *Trends Neurosci.* 19:292–297.

Juusola, M., and R.C. Hardie. 2001a. Light adaptation in *Drosophila* photoreceptors. I. Response dynamics and signaling efficiency at 25°C. *J. Gen. Physiol.* 117:3–25.

Juusola, M., and R.C. Hardie. 2001b. Light adaptation in *Drosophila* photoreceptors: II. Rising temperature increases the bandwidth of reliable signaling. *J. Gen. Physiol.* 117:27–42.

Juusola, M., E. Kouvalainen, M. Järvilehto, and M. Weckström. 1994. Contrast gain, signal-to-noise ratio, and linearity in light-adapted blowfly photoreceptors. *J. Gen. Physiol.* 104:593–621.

Juusola, M., R.O. Uusitalo, and M. Weckström. 1995. Transfer of graded potentials at the photoreceptor-interneuron synapse. *J. Gen. Physiol.* 105:117–148.

Kaneko, A. 1979. Physiology of the retina. *Annu. Rev. Neurosci.* 2:169–191.

Kawasaki, F., M. Hazen, and R.W. Ordway. 2000. Fast synaptic fatigue in *shibire* mutants reveals a rapid requirement for dynamin in synaptic vesicle membrane trafficking. *Nat. Neurosci.* 3:859–860.

Kirschfeld, K. 1967. The projection of the optical environment on the screen of the rhabdomere in the compound eye of *Musca*. *Exp. Brain Res.* 3:248–270.

Kirschfeld, K. 1976. The resolution of lens and compound eyes. *In* Neural Principles in Vision. F. Zettler and R. Weiler, editors. Springer, New York. 354–370.

Kitamoto, T. 2001. Conditional modification of behavior in *Drosophila* by targeted expression of a temperature-sensitive *shibire* allele in defined neurons. *J. Neurobiol.* 47:81–92.

Laughlin, S.B., J. Howard, and B. Blakeslee. 1987. Synaptic limitations to contrast coding in the retina of the blowfly *Calliphora*. *Proc. R. Soc. Lond. B. Biol. Sci.* 231:437–467.

Marmarelis, P.Z., and V.Z. Marmarelis. 1978. Analysis of physiological systems: the white noise approach. Plenum Publishing Corporation, NY. 487 pp.

Meinertzhagen, I.A. 1993. The synaptic population of the fly's optic neuropile and their dynamic regulation-parallels with the vertebrate retina. *Prog. Retinal Res.* 12:13–39.

Meinertzhagen, I.A., and S.D. O'Neil. 1991. Synaptic organization of columnar elements in the lamina of the wild type in *Drosophila melanogaster*. *J. Comp. Neurol.* 305:232–263.

Meinertzhagen, I.A., and K.E. Sorra. 2001. Synaptic organization in the fly's optic lamina: few cells, many synapses and divergent microcircuits. *Prog. Brain Res.* 131:53–69.

Poodry, C.A., L. Hall, and D.T. Suzuki. 1973. Developmental properties of *shibire*: a pleiotropic mutation affecting larval and adult locomotion and development. *Dev. Biol.* 32:373–386.

Rajaram, S., R.L. Scott, and H.A. Nash. 2005. Retrograde signaling from the brain to the retina modulates the termination of the light response in *Drosophila*. *Proc. Natl. Acad. Sci. USA.* 102:17840–17845.

Shannon, C.E. 1948. A mathematical theory of communication. *Bell Syst Tech J.* 27:379–423.

Shaw, S.R. 1984. Early visual processing in insects. *J. Exp. Biol.* 112:225–251.

Sinakevitch, I., and N.J. Strausfeld. 2004. Chemical neuroanatomy of the fly's movement detection pathway. *J. Comp. Neurol.* 468:6–23.

Srinivasan, M.V., S.B. Laughlin, and A. Dubs. 1982. Predictive coding: a fresh view of inhibition in the retina. *Proc. R. Soc. Lond. B. Biol. Sci.* 216:427–459.

Srinivasan, M.V., R.B. Pinter, and D. Osorio. 1990. Matched filtering in the visual system of the fly: large monopolar cells of the lamina are optimized to detect moving edges and blobs. *Proc. R. Soc. Lond. B. Biol. Sci.* 240:279–293.

Stavenga, D.G. 2003. Angular and spectral sensitivity of fly photoreceptors. II. Dependence on facet lens F-number and rhabdomere type in *Drosophila*. *J. Comp. Physiol. [A].* 189:189–202.

Sterling, P. 1983. Microcircuitry of the cat retina. *Annu. Rev. Neurosci.* 6:149–185.

Uusitalo, R.O., M. Juusola, E. Kouvalainen, and M. Weckström. 1995. Tonic transmitter release in a graded potential synapse. *J. Neurophysiol.* 74:470–473.

van der Bliek, A.M., and E.M. Meyerowitz. 1991. Dynamin-like protein encoded by the *Drosophila shibire* gene associated with vesicular traffic. *Nature.* 351:411–414.

van Hateren, J.H. 1992. Theoretical predictions of spatiotemporal receptive-fields of fly LMCs, and experimental validation. *J. Comp. Physiol. [A].* 171:157–170.

van Hateren, J.H. 1997. Processing of natural time series of intensities by the visual system of the blowfly. *Vision Res.* 37:3407–3416.

van Hateren, J.H., and H.P. Snippe. 2001. Information theoretical evaluation of parametric models of gain control in blowfly photoreceptor cells. *Vision Res.* 41:1851–1865.

van Kleef, J., A.C. James, and G. Stange. 2005. A spatiotemporal white noise analysis of photoreceptor responses to UV and green light in the dragonfly median ocellus. *J. Gen. Physiol.* 126:481–497.

Wässle, H. 2004. Parallel processing in the mammalian retina. *Nat. Rev. Neurosci.* 5:747–757.

Weckström, M., M. Järvilehto, and K. Heimonen. 1993. Spike-like potentials in the axons of nonspiking photoreceptors. *J. Neurophysiol.* 69:293–296.

Wolfram, V., and M. Juusola. 2004. Impact of rearing conditions and short-term light exposure on signaling performance in *Drosophila* photoreceptors. *J. Neurophysiol.* 92:1918–1927.

Yasuyama, K., T. Kitamoto, and P.M. Salvaterra. 1996. Differential regulation of choline acetyltransferase expression in adult *Drosophila melanogaster* brain. *J. Neurobiol.* 30:205–218.